

# The effect of temperature correction on the measured thickness of formaldehyde zones in diffusion flames for 355 nm excitation

Dimitrios C. Kyritsis, Vito S. Santoro, Alessandro Gomez

769

**Abstract** The temperature dependent corrections of the formaldehyde laser induced fluorescence raw signal are discussed for the 355 nm excitation, which is widely available as the third harmonic of Nd-YAG lasers. The temperature dependence of the HCHO partition function is calculated explicitly and the effect of quenching corrections is discussed in view of the absence of experimental data on collision cross-sections. Particular reference is made to the case of HCHO layers in hydrocarbon diffusion flames. It is shown that the thickness of such layers is not affected drastically by the calculated corrections, which has implications for the estimate of the scalar dissipation rate in diffusion flames.

## 1 Introduction

Formaldehyde (HCHO) is a relatively long-lived combustion intermediate that appears in the initial step of the  $\text{HCHO} \rightarrow \text{HCO} \rightarrow \text{CO}$  oxidation path of the combustion of hydrocarbons, alcohols and ethers (Harrington and Smyth 1993). The UV spectroscopy of this polyatomic molecule has been studied in detail by Dieke and Kistiakowski (1934), Moule and Walsh (1975) and Clouthier and Ramsay (1983). Typically the strong vibronic  $A - X \ 4_0^1$  band is excited with wavelengths in the area of 330–370 nm. Extraction of quantitative information on HCHO number density is difficult because of the strong dependence of the HCHO partition function on temperature. This problem was discussed by Klein-Douwle et al. (2000) who proposed

excitation wavelengths for which this temperature dependence is mild. Excitation with those wavelengths involves expensive, tunable dye lasers. In this short communication, we are considering excitation with the third harmonic of the Nd-YAG (355 nm), which is by now an indispensable tool in laboratories of reactive flow diagnostics. Several issues regarding this excitation were addressed in a recent study by Brackmann et al. (2003). Here we will focus on temperature corrections, with a particular emphasis on their effect on the thickness of HCHO layers.

The location and thickness of HCHO layers relate directly to significant features of combustion physics. Paul and Najm (1998) used an overlap of HCHO and OH signals to measure heat release rate and we have recently shown that the HCHO zone thickness can yield a relative measurement of the scalar dissipation rate at the stoichiometric surface ( $\chi_{\text{stoich}}$ ), which is the quantity that controls extinction of diffusion flamelets in unsteady flow fields (Santoro et al. 2000). The principle of this measurement stems from the definition of the scalar dissipation rate, which shows that this quantity scales as the inverse square of an appropriately defined thickness of the mixing layer:

$$\chi_{\text{stoich}} = 2D|\nabla Z|_{\text{stoich}}^2 \propto 1/\delta_{\text{ML}}^2, \quad (1)$$

where  $D$  is diffusivity,  $|\nabla Z|_{\text{stoich}}$  the modulus of the mixture fraction gradient at the stoichiometric surface, and  $\delta_{\text{ML}}$  is an appropriately defined thickness of the mixing layer. In our previous work, we explain in detail why the HCHO zone is a good indicator of the mixing layer and show that a measurement based on HCHO zone thickness can be more accurate than a direct measurement of  $\chi_{\text{stoich}}$  because of error accumulation in the Raman measurements involved (Bijula and Kyritsis 2004). If the appropriate temperature corrections do not affect the thickness of HCHO layers drastically, raw 2D HCHO images can be used for the relative measurement of  $\chi_{\text{stoich}}$ .

## 2 Experimental apparatus

The third harmonic of the Nd-YAG laser employed in this study had a frequency of  $28,195.49 \text{ cm}^{-1}$  with a linewidth of approximately  $1 \text{ cm}^{-1}$  (according to the manufacturer's specifications). The transition excited at this wavelength was  $\tilde{A}^2A_1 \leftarrow \tilde{X}^1A_1 \ 4_0^1 \text{ pQ}(J'' = 15, K'' = 5)$ . The laser beam was focused to an approximately 1 cm tall, 500  $\mu\text{m}$  thick sheet with a 200 mm anti-reflectively coated cylindrical

Received: 9 January 2004 / Accepted: 26 July 2004  
 Published online: 18 August 2004  
 © Springer-Verlag 2004

D.C. Kyritsis (✉)  
 Department of Mechanical and Industrial Engineering,  
 University of Illinois at Urbana-Champaign,  
 1206 W. Green Street, Urbana, IL 61801, USA  
 E-mail: kyritsis@uiuc.edu  
 Tel.: +1-217-3337794  
 Fax: +1-217-2446534

V.S. Santoro  
 Barclays S.A., London, UK

A. Gomez  
 Yale Center for Combustion Studies,  
 New Haven, CT06511, USA

The authors would like to acknowledge Mr K. Bijula of UIUC/MIE Dept. for providing data for the revised version of this note.

lens and shone through a flat, counterflow, N<sub>2</sub> diluted, CH<sub>4</sub>-O<sub>2</sub> diffusion flame. The flames and the experimental apparatus are described in detail by Bijjula and Kyritsis (2004) and Santoro et al. (2000). 2D measurements of HCHO were acquired using an ICCD camera and a narrow bandpass filter centered at 415 nm with a full width at half maximum of 7 nm, which was used to reject flame luminescence and other interferences. The laser sheet profile was monitored by imaging the fluorescence through a cell containing a uniform HCHO concentration and the appropriate corrections were applied.

### 3 Results and discussion

#### 3.1 Temperature corrections

The LIF yield in the linear regime is:

$$F = C_{\text{exp}} B_{12} N_1^0 I_v f_1 \frac{A_{21}}{A_{21} + Q_{21}} \quad (2)$$

where  $C_{\text{exp}}$  is an experimentally derived constant,  $B_{12}$  the Einstein coefficient of absorption,  $A_{12}$  the Einstein coefficient of spontaneous emission,  $I_v$  the laser spectral irradiance,  $N_1^0$  the total HCHO number density,  $Q_{21}$  the quenching rate and  $f_1$  the population fraction of the “ground state” for the particular excitation. This expression assumes that the laser line spectral profile encompasses fully the shape of the excited line and that there is no effect caused by line broadening of either the particular line under consideration or neighboring lines. The results of Dieke and Kistiakowski (1934) indicate that the closest spectral line to the one we are considering is 4 cm<sup>-1</sup> and the measurements of the excitation spectrum reported by Brackmann et al. (2003) show clearly distinct rotational lines although there is some shape overlap. Using Gaussian curve fits to the line shapes reported by Brackmann, we estimate that 10% of the signal from our excitation may be due to line overlap. We will neglect this contribution in the following analysis. As we will show, the corrections we discuss here will not prove significant for the determination of an appropriately defined thickness of the HCHO zone. The substance of this conclusion will not change because of line shape overlap. The line width caused by Doppler broadening is  $\Delta\nu_T = \nu_o/c \cdot (8kT \ln 2/m)^{1/2} = 1.12 \times 10^8 T^{1/2}$  Hz (where  $\nu_o$  is the excitation frequency,  $T$  the temperature in K,  $k$  the Boltzmann constant, and  $m$  the molecular mass), which is smaller than the laser line bandwidth for  $T < 2000$  K. The linewidth caused by homogeneous broadening is expected to be on the order of 0.1 cm<sup>-1</sup> at 300 K, 1 bar (Eckbreth 1987, p 74), an expectation that is confirmed by the measurements of Barry et al. (2003). Because these are isobaric flames, the pressure dependence of homogeneous broadening does not pose a concern. If we assume that homogeneous broadening is mainly due to collisions, we expect the corresponding linewidth to decrease with increasing temperature and be always smaller than the 1 cm<sup>-1</sup> linewidth of the laser.

We assumed decoupled energy modes ( $f_1 = f_{\text{ele}} f_{\text{vib}} f_{\text{rot}}$  where  $f$  is the population fraction given by Boltzmann statistics) and neglected the population of electronically excited states ( $f_{\text{ele}} = 1$ ). The vibrational contribution to the population fraction is:

$$f_{\text{vib}} = e^{-\nu h c \omega / kT} \left( 1 - e^{-h c \omega / kT} \right) \quad (3)$$

with  $\omega = \omega_4 = 1167$  cm<sup>-1</sup> (Clouthier and Ramsay 1983) and  $\nu = 0$ , we get:

$$f_{\text{vib}} = \left( 1 - e^{-1680.5/T} \right) \quad (4)$$

The rotational contribution is:

$$f_{\text{rot}} = \frac{(2J+1)e^{-[BJ(J+1)+(A-B)K^2]hc/(kT)}}{\sum_{J=0}^{\infty} \sum_{K=-J}^{+J} (2J+1)e^{-[BJ(J+1)+(A-B)K^2]hc/(kT)}} \quad (5)$$

where  $A$  and  $B$  the rotational constants. Following the classical approximation of Herzberg (1991), the rotational partition function denominator of Eq. 6 is:

$$Z = e^{Bhc/(4kT)} \sqrt{\frac{\pi}{B^2 A}} \left( \frac{kT}{hc} \right)^3 \times \left[ 1 + \frac{1}{12} \left( 1 - \frac{B}{A} \right) \frac{Bhc}{kT} + \frac{7}{480} \left( 1 - \frac{B}{A} \right)^2 \left( \frac{Bhc}{kT} \right)^2 + \dots \right] \quad (6)$$

where  $A = 9.45$  cm<sup>-1</sup>,  $B = 1.295$  cm<sup>-1</sup> (Clouthier and Ramsay 1983) and, for the particular transition,  $K = 5$ ,  $J = 15$ . So, Eq. 5 yields

$$f_{\text{rot}} = \frac{40.1969e^{-740/T}}{(1 + 0.134/T + 0.037/T^2)T^{3/2}} \quad (7)$$

with  $T$  in K.

For the calculation of the quenching coefficient one should in principle use

$$Q_{21} = \sum_i N_i \sigma_i \nu_i, \quad (8)$$

where  $N_i$  is the number density of the collision partner,  $\sigma_i$  the collision cross-section, and  $\nu_i$  the relative velocity of the collision partner and the excited molecule. Direct measurements of collision cross-sections are not available for excited HCHO. Shin et al. (2001) measured effective fluorescence lifetimes for excitation in the vicinity of 339 nm, and showed that they varied only  $\pm 20\%$  in the 600–1300 K range. However, caution should be exercised in transferring these conclusions to a different excitation wavelength. The approach of Paul and Najm (1998) is a more fruitful one. They assumed a  $\sigma \sim T^\beta$  dependence of the cross-section and investigated the effect of the variation of the exponent  $\beta$  in their results, by examining the two limits of  $\beta = 0$  and  $\beta = -0.5$ . Given that the  $N_i \nu_i$  term in Eq. 8 scales as  $T^{-0.5}$ , this would yield a scaling for the quenching rate that varies between  $Q_{12} \sim T^{-0.5}$  and  $Q_{12} \sim T^{-1}$ .

### 3.2

#### Effect of the proposed corrections on the thickness of HCHO zones

Figure 1 shows the correction owing to Boltzmann statistics, the quenching correction, and the total correction calculated as the product of these two corrections for  $Q_{12} \sim T^{-0.5}$  and  $Q_{12} \sim T^{-1}$ . The corrections on the raw HCHO signal can be significant, approaching a factor of 2 in the case of  $Q_{12} \sim T^{-1}$  and 1800 K. These results are in agreement with the results of Paul and Najm (1998) who used spectroscopic modeling to predict the necessary correction for a general excitation and corroborate the fact that the quenching cross-section correction should vary between the two limit cases we examined.

It is interesting, however, to notice that these significant corrections do not seem to affect drastically the thickness of the HCHO zones as the results of Fig. 2 show. There, normalized HCHO profiles are presented along with the temperature profile across a diffusion flamelet for both the cases  $\sigma = \text{const}$  and  $\sigma \sim T^{-0.5}$ . The HCHO profiles were acquired from 2D LIF data. The temperature was measured by measuring the number densities of main species with line Raman and calculating the temperature as  $T = P/nR$ , where  $P$  is the ambient pressure,  $n$  the total number density, and  $R$  the gas constant. The technique is discussed by Kyritsis et al. (2002). If  $\delta_{ML}$  in Eq. 1 is approximated as the FWHM of the profiles of Fig. 2, an error of approximately 10% would be introduced by not applying the correction to the raw HCHO data, which, from Eq. 1 would translate to a 20% error in the measurement of  $\chi_{\text{stoich}}$ . This is comparable to some of the direct, multispecies

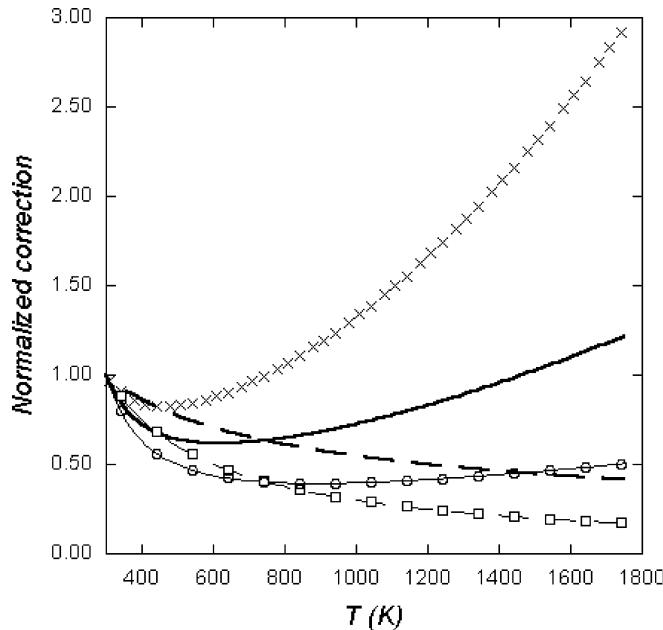


Fig. 1. Correction coefficients as a function of temperature normalized with respect to their value at  $T = 300$  K: a correction owing to the temperature dependence of the partition function (cross); b quenching correction assuming  $Q_{12} \sim T^{-0.5}$  (dashed line); c total correction assuming  $Q_{12} \sim T^{-0.5}$  (solid line); d quenching correction assuming  $Q_{12} \sim T^{-1}$  (open square); e total correction assuming  $Q_{12} \sim T^{-1}$  (open circle)

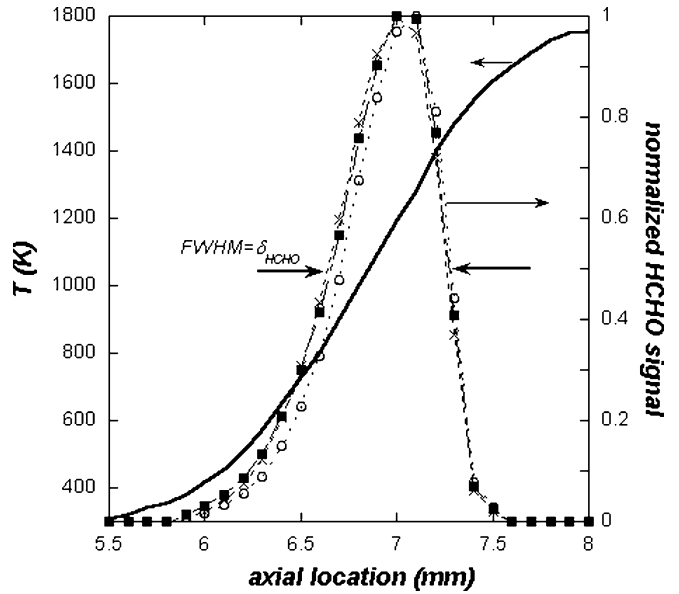


Fig. 2. Temperature distribution (solid line) and normalized HCHO profiles across a  $\text{CH}_4\text{-O}_2$ , flat, counterflow,  $\text{N}_2$  diluted, diffusion flame. Raw (uncorrected) profiles (solid square) are compared with profiles corrected with the assumption  $Q_{12} \sim T^{-1}$  (cross) and with the assumption  $Q_{12} \sim T^{-0.5}$  (open circle). The thickness of the HCHO zone is defined as full width at half maximum (FWHM)

measurements of  $\chi_{\text{stoich}}$  because of the significant error in the Raman measurements involved. Given the significant experimental resources that are required for an accurate measurement of  $\chi_{\text{stoich}}$  (Karpets et al. 2004), an estimate based on the raw thickness of the HCHO zones is a relatively inexpensive alternative, widely available to experimentalists and reasonably accurate. A serious limitation of this approach, however, is that the thickness of these layers is quite high (1.5–2 mm in Fig. 2). In a turbulent flow field, these zones may not be able to “wrinkle” around the smallest turbulent scales and the signal may survive too long as compared to some characteristic time of turbulent fluctuations.

The reason for which the effect of these corrections on the thickness of the HCHO zones is relatively mild can be seen from Figs. 1 and 2. Figure 2 shows that HCHO forms in the relatively low temperature region of the flame. The bulk of the HCHO profile lies in the 700–1300 K region. From Fig. 1, it can be seen that the corrections for such temperatures do not vary drastically with  $T$ . If  $Q_{12} \sim T^{-1}$ , the correction factor is practically constant and has no effect in the determination of the profile thickness. A slight variation with  $T$  for  $Q_{12} \sim T^{-0.5}$  causes a decrease in thickness on the order of 10%. The heart of the matter is that the local minimum in the Boltzmann correction forces the total correction to remain in the vicinity of unity for any reasonable assumption regarding the dependence of  $Q_{12}$  on  $T$ . It is interesting to see how the thickness of the HCHO zones varies with the strain rate  $K$  imposed on a steady diffusion flame. In such flames  $K$  is proportional to  $\chi_{\text{stoich}}$  (Williams 1985). So, from Eq. 1, a proportionality of the HCHO zone thickness to the inverse square root of  $K$  is expected. This theoretical expectation is shown as dashed

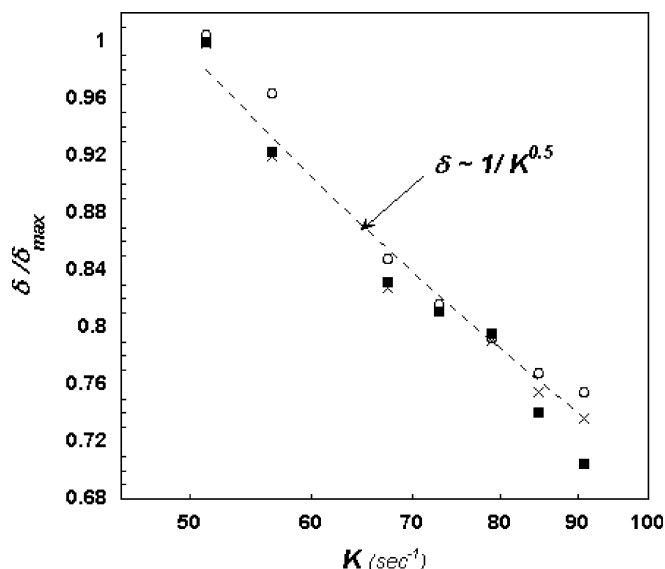


Fig. 3. Dependence of the HCHO layer thickness on strain rate for a steady, flat diffusion flame. Raw (uncorrected) profiles (solid square) are compared with profiles corrected with the assumption  $Q_{12} \sim T^{-1}$  (cross) and with the assumption  $Q_{12} \sim T^{-0.5}$  (open circle). The arbitrarily placed dashed line shows the theoretically expected inverse square-root dependence

lines on the logarithmic plot of Fig. 3. The exact placement of this line is unimportant, only its slope is. The strain  $K$  was calculated as

$$K = \frac{2U_{\text{ox}}}{L} \left[ 1 + \frac{U_{\text{F}}}{U_{\text{ox}}} \left( \frac{\rho_{\text{F}}}{\rho_{\text{ox}}} \right)^{1/2} \right]$$

where  $L$  is the distance between the two nozzles,  $U$  denotes flow speed,  $\rho$  the density and the subscripts F and ox the fuel and oxidizer stream respectively. The applied corrections do improve the agreement with the theoretically expected behavior, but not drastically. For the purposes of a relative measurement of  $\chi_{\text{stoich}}$ , the raw, uncorrected data can be used without significant loss of accuracy.

#### 4

##### Conclusions

The temperature corrections accounting for Boltzmann population distribution and quenching on HCHO signals acquired with the widely available third harmonic of the Nd-YAG laser as an excitation source can be significant for combustion temperatures. A Boltzmann correction by a factor of three is necessary at a temperature of 1800 K. There are no experimental data for quenching cross-sections, so depending on the modeling

assumptions, there can be a significant quenching correction as well. However, the effect of these corrections on the thickness of HCHO zones in diffusion flames is modest. The thickness of the corrected profiles differs only approximately 10% from the one of the raw profiles. This means that HCHO zones can be used to record scalar dissipation rates with a 20% accuracy in laminar diffusion flames, which may be a reasonable approximation in a series of applications given the experimental resources that are necessary for an accurate direct measurement of  $\chi_{\text{stoich}}$ .

##### References

- Barry HR, Corner L, Hancock G, Peverall R, Ranson TL, Ritchie GAD (2003) Measurements of pressure broadening coefficients of selected transitions in the  $2\nu_5$  band of formaldehyde. *Phys Chem Chem Phys* 5:3106–3112
- Bijjula K, Kyritsis DC (2004) Experimental evaluation of flame observables for simplified scalar dissipation rate measurements in laminar diffusion flamelets. *Proc Combust Inst* (in press)
- Brackmann C, Nygren J, Bai X, Li Z, Bladh H, Axelsson B, Denbratt I, Koopmans L, Bengtsson P-E, Aldén M (2003) Laser-induced fluorescence of formaldehyde in combustion using third harmonic Nd:YAG laser excitation. *Spectrochim Acta A* 59:3347–3356
- Clouthier DJ, Ramsay DA (1983) The spectroscopy of formaldehyde and thioformaldehyde. *Ann Rev Phys Chem* 34:31–58
- Dieke GH, Kistiakowski GB (1934) Ultraviolet absorption spectrum of formaldehyde. *Phys Rev* 45:4–44
- Eckbreth AC (1987) *Laser diagnostics for combustion, temperature and species*. Abacus Press, Cambridge, MA
- Harrington JE, Smyth KC (1993) Laser-induced measurements of formaldehyde in a methane/air diffusion flame. *Chem Phys Lett* 202:196–202
- Herzberg G (1991) *Molecular spectra and molecular structure*. Krieger, Malabar, FL
- Karpetis AN, Settersten TB, Schefer RW, Barlow RS (2004) Laser imaging system for determination of three-dimensional scalar gradients in turbulent flames. *Opt Lett* 29:355–357
- Klein-Douwle RJH, Luque J, Jeffries JB, Smith GP, Crosley DR (2000) Laser induced fluorescence of formaldehyde hot bands in flames. *Appl Opt* 39:3712–3715
- Kyritsis DC, Santoro VS, Gomez A (2002) Quantitative scalar dissipation rate measurements in vortex-perturbed counterflow diffusion flames. *Proc Combust Inst* 29:1679–1685
- Moule DC, Walsh AD (1975) Ultraviolet spectra and excited states of formaldehyde. *Chem Rev* 75:67–83
- Paul PH, Najm HN (1998) Planar laser-induced fluorescence imaging of flame heat release rate. *Proc Combust Inst* 27:43–50
- Santoro VS, Kyritsis DC, Gomez A (2000) An experimental study of vortex flame interaction in counterflow spray diffusion flames. *Proc Combust Inst* 28:1023–1030
- Shin DI, Dreier T, Wolfrum J (2001) Spatially resolved absolute concentration and fluorescence-lifetime determination of  $\text{H}_2\text{CO}$  in atmospheric-pressure  $\text{CH}_4/\text{air}$  flames. *Appl Phys B* 72:257–261
- Williams FA (1985) *Combustion theory*. Addison-Wesley, Redwood City, CA